Proceedings of the
Annual Stability Conference
Structural Stability Research Council
Louisville, Kentucky, April 1-4, 2025

Seismic design of partially concrete-filled steel tubular columns

Iraj H. P. Mamaghani[1]

Abstract
Thin-walled steel tubular columns with circular sections are widely employed as cantilever piers in bridges due to their geometric efficiency, aesthetic appeal, and excellent earthquake resistance. However, their structural integrity is often undermined by local buckling, global buckling, or a combination of both, which can lead to a significant reduction of strength and eventual collapse. This study examines the structural performance of thin-walled tubular columns with circular sections and their partially concrete-filled counterparts under constant axial and cyclic lateral loads. A detailed finite element model (FEM) was developed, accounting for both material and geometric nonlinearities. The FEM was validated against experimental data from the literature, ensuring its reliability. The validated model was further utilized in an extensive parametric study to evaluate and optimize the height of the concrete infill. The results reveal that partially filling the hollow steel tubes with concrete—up to 30-50% of the column height—substantially improves their strength, ductility, and post-buckling performance. These findings underscore the potential of partially concrete-filled tubular columns as a cost-effective and resilient solution for applications demanding enhanced structural robustness and seismic resistance.

Keywords: Local buckling, Thin-walled steel tubular columns, Concrete-filled, Cyclic behavior, Finite element analysis (FEA), Strength, Ductility, Seismic design

1. Introduction

Civil engineering structures in seismically active regions face heightened risks due to the extreme uncertainties of severe earthquakes (Miller 1998, Mahin 1998, Nakashima et al. 1998). Thin-walled steel tubular columns with circular cross sections are extensively used in modern construction, including buildings, offshore platforms, elevated storage tanks, and transmission towers. Additionally, they are often employed as cantilever piers in bridges and as structural supports for wind turbines in seismic regions, thanks to their geometric efficiency, aesthetic appeal, and superior earthquake resistance (Ucak & Tsopelas 2014, Njiru & Mamaghani 2024).
Compared to reinforced concrete columns, thin-walled steel tubular columns offer several advantages, including higher stiffness-to-cross-sectional area ratios, reduced weight, and exceptional ductility—particularly beneficial in applications where limited construction space is a

[1] Associate Professor, University of North Dakota, USA, iraj.mamaghani@und.edu

constraint. However, their performance is often compromised by local buckling, global buckling, or the interaction of both, leading to significant reductions in strength and ductility. Under cyclic lateral loading, these vulnerabilities can ultimately fail the column (Mamaghani 2004).

Observations from major earthquakes, such as the Kobe earthquake (1995), the Sichuan earthquake (2008), and the East Japan earthquake (2011), have highlighted the susceptibility of thin-walled structures to damage when subjected to cyclic lateral forces, see Fig. 1. Severe local buckling and inelastic deformation in steel bridge piers have been extensively documented (Bruneau 1998). Consequently, numerous experimental and analytical studies have been conducted to identify methods for enhancing the ductile behavior of these structures under combined axial and cyclic lateral loading.

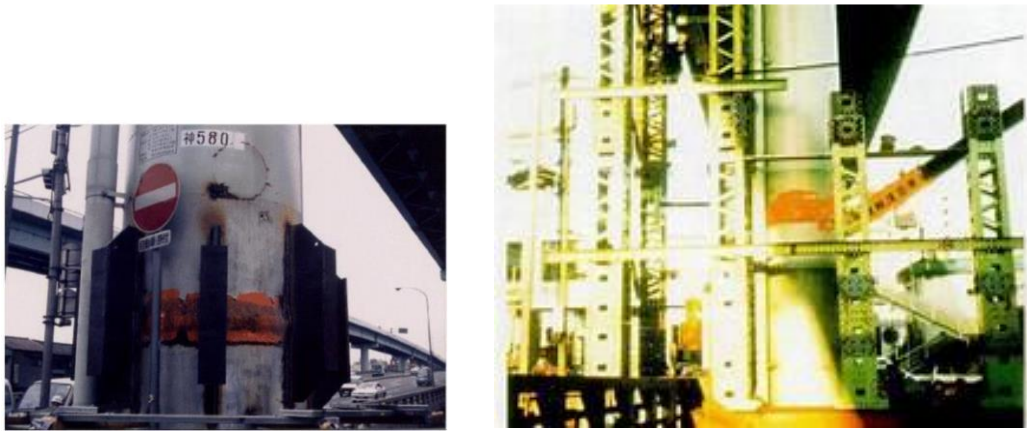

(a) (b)

Figure 1: Damaged thin-walled steel tubular bridge piers during the 1959 Kobe earthquake in Japan. (a) Local buckling observed near the base of a hollow circular bridge pier, (b) Local buckling at the hollow section above the infill concrete level in a partially concrete-filled circular pier

For instance, Usami et al. (1995) and Usami & Ge (1998) conducted numerical studies to evaluate factors influencing the strength and ductility of circular sections. Gao et al. (1998a, 1998b) utilized finite element (FE) analysis to demonstrate that the ductility of circular sections is highly sensitive to the radius-to-thickness ratio (R/t). Reducing both the R/t ratio and the column slenderness ratio (λ) significantly improved strength and ductility. Experimental research on retrofitting circular cross sections (Nishikawa et al. 1998, Mamaghani 2004) concluded that retrofitting strategies such as longitudinal stiffeners, diaphragms, corner reinforcements, corner plates, and concrete infill can markedly enhance strength and ductility. Moreover, new thin-walled corrugated and cellular steel column designs introduced by Ucak & Tsopelas (2006) have demonstrated superior strength, ductility, and buckling resistance performance.

1.1 Objective and Scope

This study numerically investigates the behavior of partially concrete-filled thin-walled steel tubular columns with circular cross-sections under combined axial and cyclic lateral loading. Finite element (FE) models were developed incorporating geometric and material nonlinearities. The

results of these FE analyses were validated against experimental data from the literature to confirm the reliability of the modeling approach.

Additionally, partially concrete-filled thin-walled steel tubular columns were analyzed to improve hollow columns' strength, ductility, and post-buckling behavior. The enhanced performance of these partially concrete-filled columns is attributed to their ability to mitigate severe local buckling near the column base, see Fig. 1(a), where buckling is most likely to occur in a hollow section.

2. Numerical Method

Full-scale testing undoubtedly provides valuable insights into the behavior of structures. However, physical experiments are often expensive and time-consuming. To address these challenges, a series of finite-element analyses (FEA) on the cyclic behavior of partially concrete-filled thin-walled steel tubular columns was conducted using the commercially available finite-element software, ABAQUS Ver. 6.14 (Hibbitt et al. 2014). The finite-element modeling (FEM) accounts for both material and geometric non-linearities, ensuring a comprehensive simulation of the columns' behavior.

The accuracy of the FEM was validated by comparing its results with experimental data reported by Nishikawa et al. 1998. The study focused on key parameters essential for the practical design of thin-walled cross-sections, including the radius-to-thickness ratio parameter of circular sections (R_t), the column slenderness ratio parameter (λ), and the height of infill concrete (h_c) (Usami et al. 1995, Mamaghani & Packer 2002).

The parameter R_t primarily influences the local buckling behavior of thin-walled steel circular columns, while λ governs their flexural stability (Mamaghani & Packer 2002, Mamaghani, 2008). These parameters are defined as follows:

$$R_t = \frac{d}{2t}\frac{\sigma_y}{E}\sqrt{3(1-v^2)} \tag{1}$$

$$\lambda = \frac{2h}{r}\frac{1}{\pi}\sqrt{\frac{\sigma_y}{E}} \tag{2}$$

Where h = column height; r = radius of gyration of the cross-section; σ_y = yield stress; E = Young's modulus; v = Poisson's ratio; d = diameter of circular cross-section; and t = plate thickness. Under the test, the column is subjected to a constant axial load of (P) and cyclic lateral displacement at the top of the column, Fig. 2b.

2.1 Partially Concrete-Filled Thin-Walled Steel Circular Columns

Thin-walled steel circular columns often experience premature buckling—manifesting as local buckling, global buckling, or a combination of both—near the column base when subjected to combined axial and cyclic lateral loading, Fig. 1a. This buckling behavior limits the ability of these columns to fully utilize their strength and ductility capacities, leading to suboptimal performance (Usami et al. 1995).

To overcome these limitations, partially concrete-filled thin-walled steel tubular columns have been proposed as an enhanced alternative to hollow columns. For a consistent comparison, both column types are designed with identical overall height and diameter.

In the partially concrete-filled columns, the height is divided into two distinct parts, see Fig. 2. The lower part, which is filled with concrete, is further divided into:

1. Segment 1: Extending from the base, with a height equal to the column's diameter, d.
2. Segment 2: Stretching to a height of $h_c - d$, where h_c represents the total height of the concrete-filled portion.

The upper part, which remains hollow, has a height of $h - h_c$, where h, is the overall column height. As illustrated in Fig. 2, the lower part of the column features a composite cross-section, integrating steel and concrete. This configuration is specifically chosen to optimize the height of the concrete infill and enhance the column's structural behavior, resulting in increased strength and ductility (Usami et al. 1995).

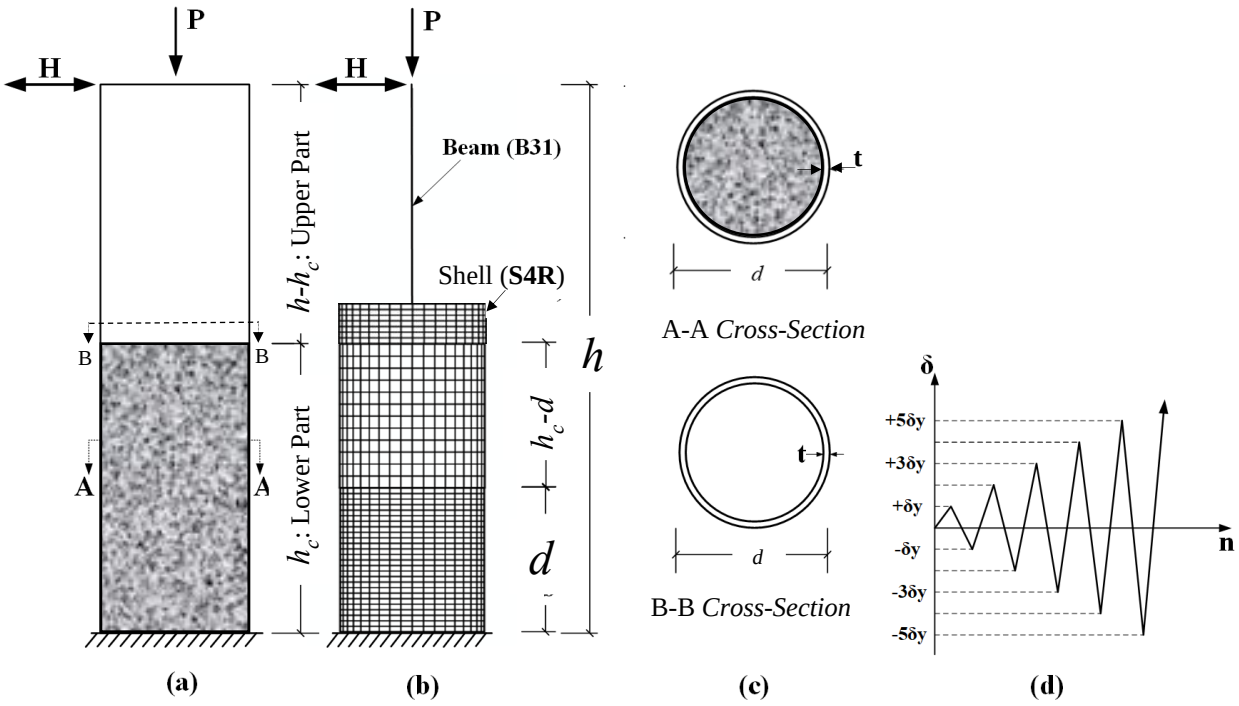

Figure 2: Analytical Model: (a) Bridge Pier, (b) FE Model, (c) Cross Sections, and (d) Loading Program

Table 1 summarizes the material and geometrical properties of the analyzed columns. Apart from the height of the concrete infill, all other properties, including material characteristics and overall dimensions are identical for both the hollow and partially concrete-filled columns. This ensures a controlled evaluation of the benefits provided by the partial concrete filling.

Table 1: Geometric and Material properties of the specimens

Properties	No.16 Column[1]		No. 30 Column[1]	
	Hollow	CFT	Hollow	CFT
Steel tube material	SS400	SS400	SS400	SS400
h (mm)	3423	3423	3423	3423
h_c *(mm)*	-	2303	-	2303
d (mm)	900	900	900	900
t (mm)	9.00	9.00	9.00	9.00
λ	0.268	0.268	0.268	0.268
R_t	0.123	0.123	0.123	0.123
Hy (KN)	443.94	443.94	400.82	400.82
δy *(mm)*	11.53	11.53	10.5	10.5
$P/\sigma_y A_s$	0.114	0.114	0.199	0.199
σ_y *(MPa)*	308.0	308.0	308.0	308.0
σ_u *(MPa)*	559.5	559.5	534	534
f'_c *(MPa)*	-	27.93	-	21.46

1. Reported in Nishikawa et al. 1998.
Note: E = 205.8 MPa, and v = 0.3 for all specimens

3. Finite Element Analysis (FEA)

3.1 Modeling of Thin-Walled Steel Tubes

Local buckling typically occurs near the base of thin-walled steel tubular columns when subjected to constant axial loads combined with cyclic lateral displacements (Nishikawa et al. 1998, Mamaghani 2004). To effectively simulate this behavior, as illustrated in Fig. 2b:

- A two-node beam element (B31) is employed for the upper part of the column, as it efficiently represents global deformation.
- A four-node shell element (S4R) is utilized for the lower part of the column to account for localized deformation, including local buckling accurately.
  The interface between the shell (S4R) and beam (B31) elements is modeled using a multi-point constraint (MPC), ensuring continuity. Both elements are readily available in the ABAQUS element library (Hibbitt et al. 2014).

The modeled cantilever column is fixed at the base and subjected to a constant axial load. At the same time, cyclic lateral displacements are applied at its top (Fig. 2b). For computational efficiency, the meshing strategy is carefully optimized through trial and error:

- The bottom segment of the lower part (d) is divided into 26 shell elements for a finer mesh to capture local buckling behavior accurately.
- The remaining height of the lower part ($h_c - d$) is divided into 14 shell elements.
- The upper part of the column is discretized into 14 beam elements.

This mesh density was found to produce accurate results while maintaining computational efficiency.

The analysis employs a displacement convergence criterion, with a tolerance level of 10^{-5}. Initial geometrical imperfections and residual stress are not considered in the simulation, as these factors were not measured in the experimental tests (Nishikawa et al. 1998). For thin-walled steel tubular columns, cyclic lateral loads have a more dominant effect than axial loads, making the influence of initial imperfections negligible (Goto et al. 1998, Mamaghani 2008).

Special attention is given to regions where local buckling is likely to occur. A finer mesh is created at:

1. The bottom part of the column, near the base where local buckling typically originates.
2. The hollow section above the top of the concrete infill, as this area is also prone to local buckling under cyclic loads (Fig. 2b).

3.2 Modeling of In-Filled Concrete

Concrete exhibits brittle behavior under tensile stresses and low compressive stresses but transitions to a ductile response under high hydrostatic pressure. Its brittle behavior diminishes when sufficient confining pressure prevents crack propagation. In conventional concrete modeling, compressive behavior is typically represented using a plasticity model, while tensile behavior is modeled with the smeared cracking approach (Chen & Chen 1971). However, the smeared cracking model often faces numerical challenges, particularly when analyzing cyclic loads.

To address this issue, this study employs the concrete-damaged plasticity model (Lee and Fenves 1998), implemented in ABAQUS (Hibbitt et al. 2014). Although this model offers a more robust approach under cyclic loading, it is less precise in capturing tensile behavior compared to the smeared cracking model, as it assumes isotropic plasticity on the tensile side. The concrete damaged plasticity model is an isotropic plasticity framework that closely resembles the Drucker-Prager model in its treatment of compressive behavior.

The model is implemented in finite-element analysis (FEA) using an eight-node solid element with reduced integration (C3D8R). The constitutive relationship for multiaxial stress states is derived based on the non-associated flow rule, using the Drucker-Prager hyperbolic flow potential function (Hibbitt et al. 2014).

The input parameters for the concrete-damaged plasticity model in ABAQUS (Hibbitt et al. 2014) are provided in Table 2. These parameters include:

E_c: Modulus of elasticity of concrete
v: Poisson's ratio
ψ: Dilation angle
e: Flow potential eccentricity
K_c: Compressive meridian
f_{bo}/f_c: Ratio of compressive strength under biaxial loading to uniaxial compressive strength
ω: Viscosity parameter

Table 2: Material parameter for concrete

Parameter	No. 16	No. 30
E_c	18670	16620
ν	0.2	0.2
ψ	38	38
e	0.2	0.2
K_c	0.7	0.7
f_{bo}/f_c	1.1	1.1
ω	0.001	0.001

To improve numerical convergence in solving contact equations, it is recommended to assign a small, nonzero value to the viscosity parameter (ω) instead of zero.

3.3. Material behavior

The hysteretic behavior of thin-walled steel tubes is strongly affected by the interaction between local buckling and cyclic metal plasticity. To accurately represent this behavior, the kinematic hardening rules provided in ABAQUS **(**Hibbitt et al. 2014) are utilized to model the material's cyclic plasticity. Material constants necessary to specify the concrete damaged plasticity model are Young's modulus E_c, Poisson's ratio v_c, and equivalent stress-equivalent strain relation for compression, and damage parameters. These parameters adopted by Goto et al. (2010) are listed in Table 2. Figs. 3a and 3b illustrate the multilinear stress-strain curve adopted for Steel SS400 and the stress-strain curve used for the compressive behavior of concrete in the finite element analysis, respectively.

Compared to reinforced concrete columns, thin-walled steel tubular columns offer several advantages, including higher stiffness-to-cross-sectional area ratios, reduced weight, and exceptional ductility—particularly beneficial in applications where limited construction space is a constraint. However, their performance is often compromised by local buckling, global buckling, or the interaction of both, leading to significant reductions in strength and ductility. Under cyclic lateral loading, these vulnerabilities can ultimately fail the column (Mamaghani 2004).

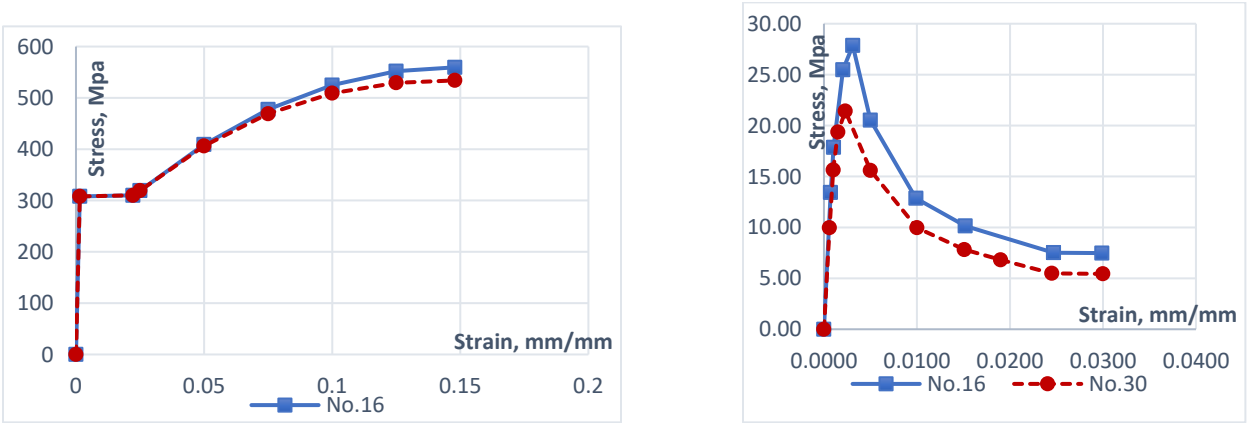

(a) (b)

Figure 3: (a) Stress-plastic strain of steel SS400, (b) Compressive stress-strain of confined concrete

3.4 Cyclic Loading Program

The schematic representation of the displacement-controlled unidirectional cyclic loading program is shown in Fig. 2d, which serves as the adopted lateral loading protocol. The unidirectional cyclic loading is applied quasi-statically at the top of the specimen, while a constant axial load (P) is maintained throughout the loading process. The displacement amplitude of the cyclic loading is incrementally increased as a multiple of the yield displacement (δ_y), defined by Eq. 3**:**

$$\delta_y = \frac{H_y h^3}{3E_s I_s} \tag{3}$$

Here, $Hy = (\sigma y - P/A)z/h$, is the lateral yield load, A is the cross-sectional area, h is the height, E_sI_s is the flexural rigidity of the hollow steel tube, and Z is the section modulus of the hollow steel tube (Goto et al. 2010). The yield displacement (δ_y) and lateral yield load (H_y) for the analyzed columns are listed in Table 1.

The analyzed columns are fabricated using carbon steel SS400 (JIS 2012), equivalent to ASTM A36 (ASTM 2014). The tubular columns are constructed from SS400 steel pipes, each containing three internal diaphragms installed at intervals of 900 mm, equal to the pipe diameter. The geometric and material parameters for the specimens are summarized in Table 1. Among these parameters, the radius-to-thickness ratio (R_t) influences the local buckling behavior of hollow columns.

The CFT column specimens No. 16 and No. 30 share the same radius-to-thickness ratio (R_t = 0.123), but they differ in their axial force ratios ($P/\sigma_y A_s$), which are 0.114 and 0.199, respectively. For comparison, the specimens with h_c = 0 are hollow columns with identical dimensions to specimens No. 16 and No. 30.

4. Results and Discussion

This section compares the numerical results of the cyclic behavior of partially concrete-filled thin-walled steel tubular columns with experimental data conducted by the Public Works Research Institute (PWRI) in Japan (Nishikawa et al. 1998).

4.1 Comparison of numerical and experimental results

Initially, the hysteresis loops from FE analysis predictions are compared with test results available in the literature (Nishikawa et al. 1998). The normalized lateral load, H/Hy, versus lateral displacement, δ/δy, hysteresis curves from the FE analysis for the partially concrete-filled specimen No. 16 show a reasonable agreement with the test results, See Fig. 4a. This indicates that FE analysis, using kinematic hardening material behavior, gives a reasonable accuracy to describe the material behavior with consideration of local buckling of thin-walled steel tubular columns. However, the specimens' stiffness with reversal loading at large lateral displacements is slightly overestimated, Fig. 3a. The reason could be attributed to some factors, such as the presence of residual stress, initial crookedness, etc. which are not considered in analytical modeling. The specimen was fabricated by wielding cold-formed steel thin plates together and this procedure left residual stress in the specimen, causing buckling at a lesser load. Initial crookedness creates additional moments in the specimen which is also responsible for buckling taking place at lower

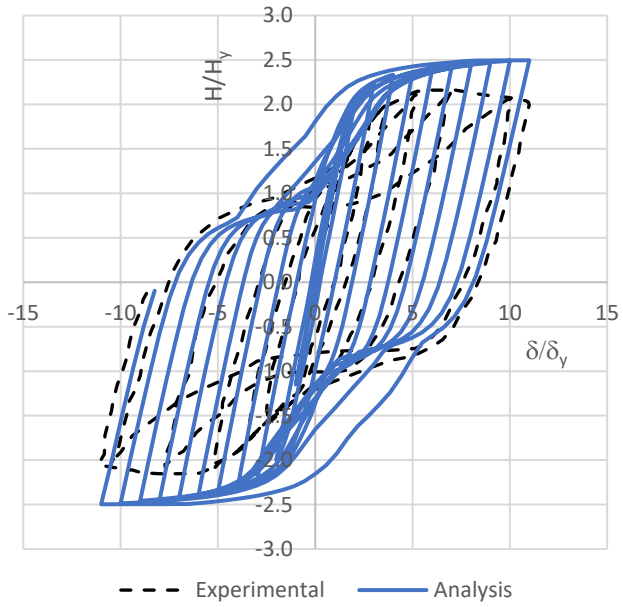

(a) Normalized lateral load versus lateral displacement at the top of the column

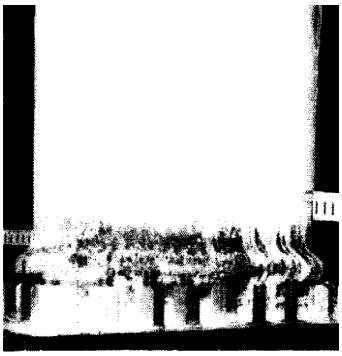

(b) buckling at the end of the test program (Nishikawa et al. 1998)

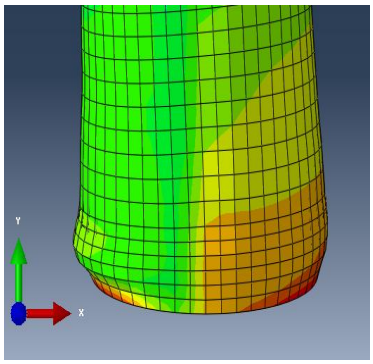

(c) Buckling at the end of the analysis

Figure 4: Comparison of the test results with finite element analysis for specimen No. 16

horizontal force. Another reason is that the kinematic hardening model does not consider the Bauschinger effect (Mamaghani et al. 1995 & 1996). Similar findings have been reported in other studies (Goto et al. 1998, Ucak & Tsopelas 2006). As shown in Figs. 4b and 4c, the deformed shapes of the column at the end of the FE analysis are compared to the deformed shapes at the end of the test (Nishikawa et al. 1998). Based on this comparison, the deformed shapes of the column are captured relatively well in the analysis.

5. Parametric Study

The specimens were further analyzed by varying the height of the concrete infill to investigate its influence on buckling behavior. Specimens No. 16 and No. 30 were examined with different infill heights to evaluate the effect of the concrete fill on column performance under cyclic loading. For

the parametric study, the ratio of the infill concrete height to the total column height (h_c/h) varied from 0% (no infill concrete) to 67%, as detailed in Table 3.

Table 3: Height of concrete infilled

h_c/h		30%	50%	53%	67%
No.16	h_c (mm)	1030	1712	1815	2303
No.30	h_c *(mm)*	1030	1712	1815	2303

The normalized hysteresis curve and column buckling pattern are used to compare the cyclic behavior of the analyzed columns. Fig. 5 illustrates the improvement in the normalized hysteresis behavior of columns with the increase in height of infill concrete, highlighting the positive impact on strength and ductility. The results indicate that columns with 30% and 50% infill exhibit enhanced strength and ductility; however, severe buckling occurs during higher loading cycles, causing a reduction in strength, see Fig. 5a and 5b. In contrast, columns with 53% or greater infill height demonstrate optimal performance, maintaining structural integrity and resisting severe buckling even under higher cycles, see stable hysteresis loops in figs. 5c and 5d. Additionally, the

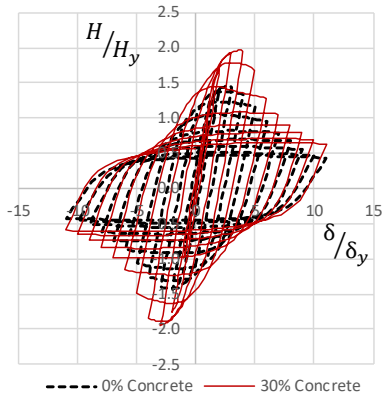

(a) h_c/h = 30%

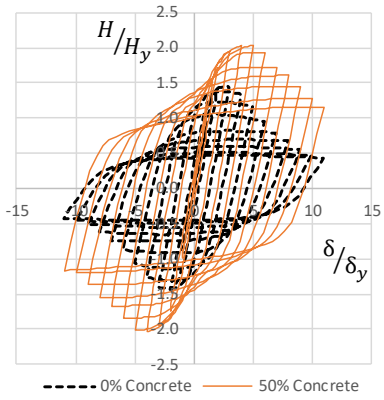

(a) h_c/h = 50%

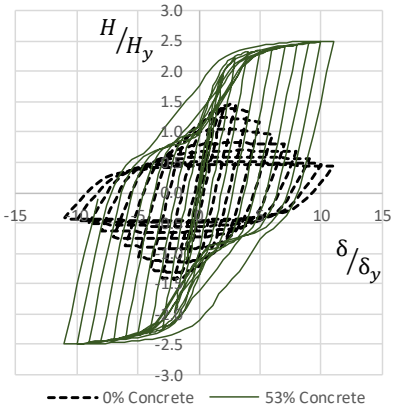

(a) h_c/h = 53%

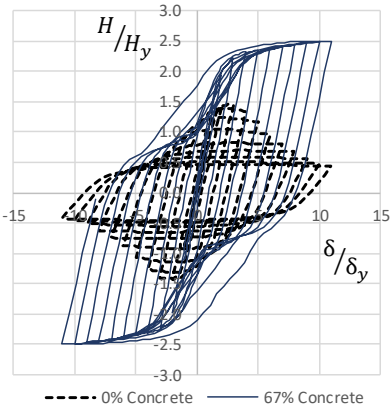

(a) h_c/h = 67%

Figure 5: Specimen No. 16: Improvement in strength and ductility for different height of infill concrete as

results in Fig. 5 reveal that increasing the infill height beyond 53% does not result in any significant improvement in strength and ductility, suggesting that 53% represents an optimal height for infill concrete in terms of balancing strength, ductility, and buckling resistance.

Figures 6(a) through 6(e) depict the local buckling patterns and locations for Specimen No. 16 under varying concrete infill heights. For the hollow column (h_c/h = 0%), severe local buckling occurs near the base, as shown in Fig. 6(a). When the infill concrete height increases to 30%-50% of the column height, local buckling shifts to the hollow section just above the concrete fill level. Among these cases, local buckling is more pronounced for h_c/h = 30% compared to h_c/h = 50%.

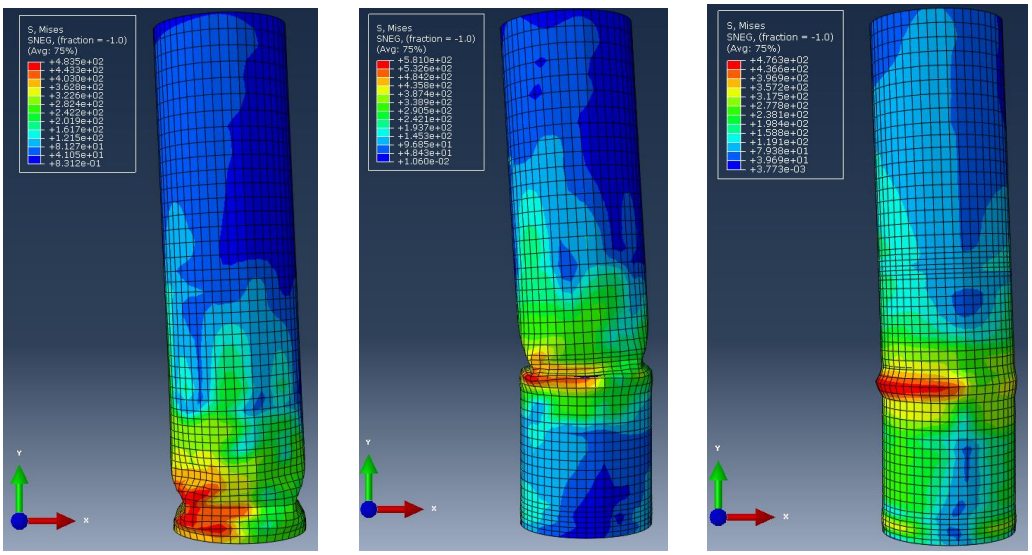

(a) h_c/h = 0% (b) h_c/h = 30% (c) h_c/h = 50%

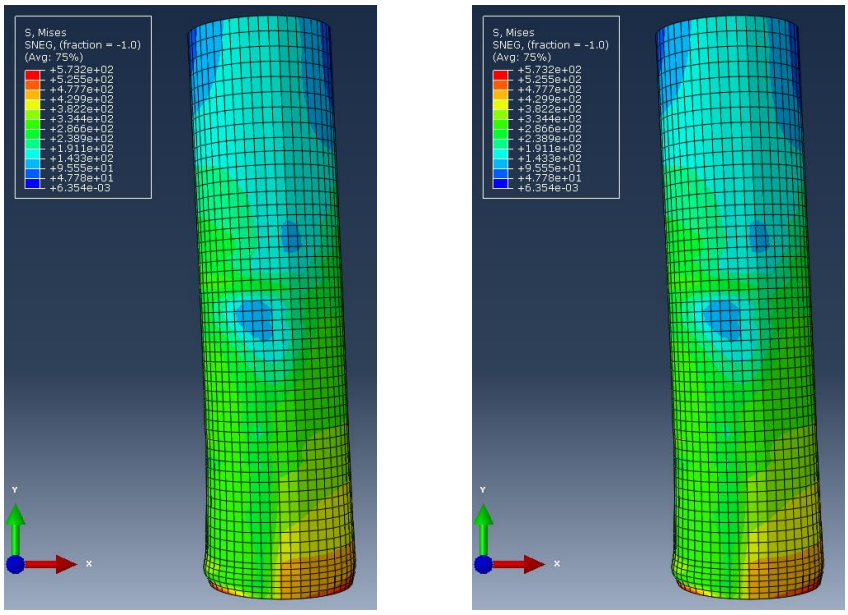

(d) h_c/h = 53% (e) h_c/h = 67%

Figure 6: Patterns of local buckling for column No. 16 at the loading point corresponding to δ/δ_y = 11

As the infill concrete height increases to 50%, local buckling continues to occur at the hollow section above the fill level but with reduced severity. When the concrete infill is further increased to 53%-67% (h_c/h = 53% and h_c/h = 67%), local buckling transitions to the composite section near the base of the column, see Figs. 6d and 6e. At these higher infill levels, buckling becomes less severe, with h_c/h = 67% exhibiting the least buckling, and no buckling is observed in the hollow section above the infill concrete.

These observations highlight that increasing the concrete height from 30% to 50% not only shifts the local buckling upward but also reduces its severity. With infilling concrete beyond 50%, local buckling transitions from the hollow section above the concrete fill to the composite section near the column base, with severity diminishing as the infill height increases. This behavior demonstrates the effectiveness of partial concrete infill in mitigating local buckling and enhancing column performance.

5.1 Effect of axial load and infill concrete height

Figures 7(a) through 7(e) illustrate the normalized hysteresis curves for Specimens No. 16 (P/P_y = 0.114) and No. 30 (P/P_y = 0.199) for varying concrete fill heights and axial load. The increase in height of concrete fill up to 50% significantly improves the strength and ductility of the column. This improvement can be described in two ways: firstly restraining buckling which provides greater stability and secondly higher energy absorption which provides greater ductility. Even though increased ductility is observed for 30% and 50% height of concrete severe buckling occurs at higher cyclic displacement causing a reduction in strength and ductility. The infill concrete beyond 53% has negligible effect on strength and ductility while it adds to the weight of the structure in turn increases the inertia force on the structure. The increase in weight of the column due to filling above 50% requires a stronger foundation to support the added weight and inertia forces due to seismic events. This observation suggests that partially filling thin-walled steel tubular columns up to 50% will be practically important as it improves the seismic resilience of the bridge piers. The results indicate no significant improvement in ductility by filling the tube with concrete beyond 53% of its height, see Figs. 7d and 7e .The hysteresis loops in Fig. 7 suggest that column No. 30 with a higher axial load (P/P_y = 0.199) exhibits a larger lateral load capacity (higher hysteresis loops) as compared to column No. 16 (P/P_y = 0.114) indicating that the larger axial load has the stabilizing effect of the partially concrete-filled columns under lateral loads.

Figures 7(a) through 7(e) present the normalized hysteresis curves for Specimens No. 16 (P/P_y = 0.) and No. 30 (P/P_y = 0.199) under varying concrete fill heights and axial loads. Increasing the concrete fill height up to 50% significantly enhances the column's strength and ductility. This improvement can be attributed to two key factors: (1) restraining local buckling, which enhances stability, and (2) increasing energy absorption capacity, which improves ductility.

Although columns with 30% and 50% concrete infill exhibit increased ductility, severe buckling occurs at higher cyclic displacements, leading to a reduction in both strength and ductility. Beyond a concrete fill height of 53%, the improvements in strength and ductility become negligible, while the additional weight increases the column's inertia forces, which may negatively impact seismic performance. The added weight also necessitates a stronger foundation to accommodate the increased mass and resulting seismic forces.

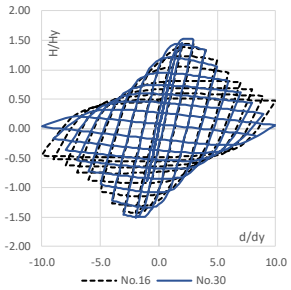

(a) hollow steel columns

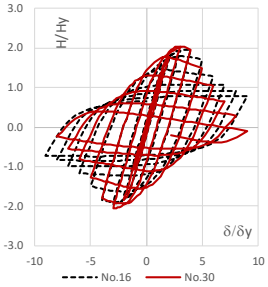

(b) 30% infill concrete

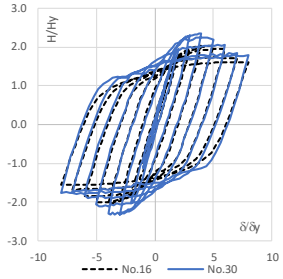

(b) 50% infill concrete

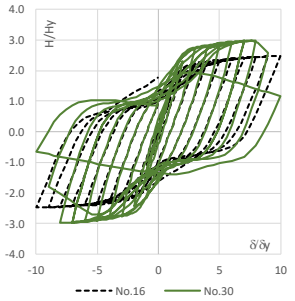

(b) 53% infill concrete

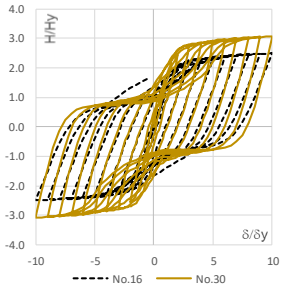

(b) 67% infill concrete

Figure 7: Comparison between hysteresis diagram for axial load and infill concrete height

These findings suggest that partially filling thin-walled steel tubular columns with concrete up to 53% of their height is an effective and practical approach to improving seismic resilience, particularly for bridge piers. Filling the column above 53% provides minimal benefits while imposing additional structural demands.

Additionally, as shown in Figs. 7(d) and 7(e), no significant improvement in ductility is observed when the concrete fill exceeds 53% of the column height. The hysteresis loops in Fig. 7 also reveal that Specimen No. 30, with a higher axial load (P/P_y = 0.199), exhibits greater lateral load capacity (larger hysteresis loops) compared to Specimen No. 16 (P/P_y = 0.114). This indicates that higher axial loads have a stabilizing effect on partially concrete-filled columns under lateral loads.

6. Conclusions

This study employed finite element (FE) analysis to investigate the cyclic behavior of partially concrete-filled thin-walled steel tubular columns with circular sections, representing bridge piers. The structural performance of hollow and partially concrete-filled columns was evaluated under

constant axial loads and cyclic lateral loads. A robust finite element model (FEM) was developed, incorporating both material and geometric nonlinearities, and validated against experimental data from the literature to ensure accuracy and reliability. The validated FEM was utilized in a comprehensive parametric study to optimize the height of the concrete infill. The findings revealed that partially filling the hollow steel tubes with concrete up to 53% of the column height significantly enhances strength, ductility, and post-buckling behavior. Increasing the concrete infill height to 50% was found to effectively shift local buckling upward to the hollow section above the concrete fill while reducing its severity. Beyond 50% infill height, local buckling transitioned to the composite section near the column base, with reduced severity as the infill height increased. However, no significant improvement in structural performance was observed for infill heights beyond 53%. These results highlight the ability of partial concrete infill to mitigate local buckling, enhance stability, and improve energy absorption capacity under cyclic loading. Moreover, the study underscores the practicality of partially concrete-filled tubular columns as a cost-effective, structurally robust, and seismically resilient solution for bridge piers and similar applications. By balancing performance improvements and material efficiency, this approach offers significant advantages in structural design for seismic regions.

References

ASTM. (2014). "ASTM A36 / A36M - 14 Standard specification for carbon structural steel." *ASTM Internatio*nal, West Conshohocken, PA: 12–14.

Bruneau, M. (1998). "Performance of steel bridges during the 1995 Hyogoken–Nanbu (Kobe, Japan) earthquake—a North American perspective." *Engineering Structures*, 20(12): 1063-1078.

Chen, W., and Chen, C. H. (1971). "Analysis of concrete-filled steel tubular beam-columns." *Engineering, Materials Science*, 33, 73-49.

Gao, S., Usami, T. & Ge, H. (1998a). "Ductility evaluation of steel bridge piers with pipe sections." *Journal of Engineering Mechanics*, 124(3): 260-267.

Gao, S., Usami, T. & Ge, H. (1998b). "Ductility of steel short cylinders in compression and bending." *Journal of Engineering Mechanics*, 124(2):176–183.

Goto, Y., Kumar, G. & Kawanishi, N. (2010). "Nonlinear finite-element analysis for hysteretic behavior of thin-walled circular steel columns with in-filled concrete." *Journal of Structural Engineering*, 136(11): 1413–1422.

Goto, Y., Wang, Q. & Obata, M. (1998). "FEM analysis for hysteretic behavior of thin-walled columns." *Journal of Structural Engineering*, 124(11): 1290–1301.

Hibbitt, Karlsson & Sorensen (2014). "Abaqus 2014 Documentation." *Dassault Systèmes*, Providence, RI, USA.

JIS. (2012). "JIS handbook: Ferrous Materials & Metallurgy." *Japanese Standards Association*.

Lee J., and Fenves, G. L. (1998). "Plastic-damage model for cyclic loading of concrete structures." *Journal of Engineering Mechanics*, Volume 124, Issue 8.

Mahin, S.A. (1998). "Lessons from damage to steel buildings during the Northridge earthquake." *Engineering Structures*, 20(4–6): 261–270.

Mamaghani, I.H.P. (2004). "Seismic design and retrofit of thin-walled steel tubular columns." *13th World Conference on Earthquake Engineering*, August 1-6, Vancouver, B.C., Canada, Paper No. 271: pp. 1-15.

Mamaghani, I.H.P. (2008). "Seismic design and ductility evaluation of thin-walled steel bridge piers of box sections." Transportation Research Record: *Journal of the Transportation Research Board*, 2050(1): 137–142.

Mamaghani, I.H.P. & Packer, J.A. (2002). "Inelastic behaviour of partially concrete-filled steel hollow sections." *In 4th Structural Specialty Conference of the Canadian Society for Civil Engineering*, Montréal, Québec, 5-8.

Mamaghani, I.H.P., Shen, C., Mizuno, E., and Usami, T. (1995). "Cyclic behavior of structural steels. I: Experiments." *Journal of Engineering Mechanics, ASCE*, USA, Vol.121, No.11, 1158-1164.

Mamaghani, I. Usami, T. & Mizuno, E. (1996). "Cyclic elastoplastic large displacement behavior of steel compression members." *Journal of structural engineering*, JSCE, Japan, 42A: 135–145.

Miller, D.K. (1998). "Lessons learned from the Northridge earthquake." *Engineering Structures*, 20(4–6): 249–260.

Nakashima, M., Inoue, K. & Tada, M. (1998). "Classification of damage to steel buildings observed in the 1995 Hyogoken-Nanbu earthquake." *Engineering Structures*, 20(6): 271–281.

Nishikawa, K., Yamamoto, S., Natori, T., Terao, K., Yasunami, H. and Terada, M. (1998). "Retrofitting for seismic upgrading of steel bridge columns." *Engineering Structures*, 20(4–6): 540–551.

Njiru, M., and Mamaghani, I.H.P. (2024). "Seismic design and ductility evaluation of thin-walled stiffened steel square box columns." MDPI, *Journal of the Applied Science*, Appl. Sci. 2024, 14(18), 8554; https://doi.org/10.3390/app14188554.

Ucak, A. & Tsopelas, P. (2006). "Cellular and corrugated cross-sectioned thin-walled steel bridge-piers/columns." *Structural Engineering and Mechanics*, 24(3): 355–374.

Ucak, A. & Tsopelas, P. (2014). "Load path effects in circular steel columns under bidirectional lateral cyclic loading." *Journal of Structural Engineering*, 141(2009): 1–11.

Usami, T. & Ge, H. (1998). "Cyclic behavior of thin-walled steel structures—numerical analysis." *Thin-walled structures*, 32(1-3): 41-80.

Usami, T., Suzuki, M., Mamaghani, I.H.P., Ge, H.B. (1995). "A proposal for check of ultimate earthquake resistance of partially concrete-filled steel bridge piers." *Journal of Structural Mechanics and Earthquake Engineering*, JSCE, Japan, No. 525/I-33, 69-82, (In Japanese).